How Electron Hydrodynamics Can Eliminate the Landauer-Sharvin Resistance

How Electron Hydrodynamics Can Eliminate the Landauer-Sharvin Resistance

Ady Stern,[1] Thomas Scaffidi,[2,3] Oren Reuven,[1] Chandan Kumar,[1] John Birkbeck,[1] and Shahal Ilani[1]
[1]Department of Condensed Matter Physics, Weizmann Institute of Science, Rehovot 76100, Israel
[2]Department of Physics and Astronomy, University of California, Irvine, California 92697, USA
[3]Department of Physics, University of Toronto, 60 St. George Street, Toronto, Ontario M5S 1A7, Canada

(Received 7 November 2021; accepted 14 September 2022; published 7 October 2022)

It has long been realized that even a perfectly clean electronic system harbors a Landauer-Sharvin resistance, inversely proportional to the number of its conduction channels. This resistance is usually associated with voltage drops on the system's contacts to an external circuit. Recent theories have shown that hydrodynamic effects can reduce this resistance, raising the question of the lower bound of resistance of hydrodynamic electrons. Here, we show that by a proper choice of device geometry, it is possible to spread the Landauer-Sharvin resistance throughout the bulk of the system, allowing its complete elimination by electron hydrodynamics. We trace the effect to the dynamics of electrons flowing in channels that terminate within the sample. For ballistic systems this termination leads to back-reflection of the electrons and creates resistance. Hydrodynamically, the scattering of these electrons off other electrons allows them to transfer to transmitted channels and avoid the resistance. Counterintuitively, we find that in contrast to the ohmic regime, for hydrodynamic electrons the resistance of a device with a given width can decrease with its length, suggesting that a long enough device may have an arbitrarily small total resistance.

DOI: 10.1103/PhysRevLett.129.157701

Introduction.—The electronic resistivity to the flow of current is a fundamental quantity in condensed matter physics. Frequently, its minimization is desired. The Drude model, dating back to 1900, suggests that the resistivity originates mostly from momentum loss to impurities. However, it was realized that even in the ballistic limit, in which impurities and phonons are absent, the interface between the electronic system and the metallic contacts to which it is coupled carries another fundamental source of resistance: the Landauer-Sharvin (LS) resistance [1–4]. This resistance is inversely proportional to the number of quantum mechanical channels that are transmitted through the system.

More recently, another regime of transport was discovered, in which electrons behave like a viscous fluid due to strong momentum-conserving electron-electron scattering [5–50]. Somewhat counterintuitively, it was shown that the resistance in this hydrodynamical regime may be lower than the ballistic one, suggesting the term "superballistic" [29,30,51–53]. Furthermore, conditions in which field-free current flow may locally exist were suggested [42].

In this Letter, using a combination of Landauer and Boltzmann analyses we demonstrate a mechanism by which electron hydrodynamics can eliminate the LS resistance, and find the minimal value that this resistance may attain. Our study is semiclassical and focuses on two dimensional systems. We describe an electronic system in terms of its conduction channels, and show that when the number of channels varies along the direction of the current flow, the Landauer-Sharvin resistance detaches from the contacts and spreads over the bulk of the electronic system. When the length scale of this spreading is larger than the electron-electron scattering mean free path, ℓ_{ee}, the resistance is dramatically suppressed.

Microscopically, this suppression results from the scattering of electrons whose channels are being terminated due to a narrowing of the system's cross section or a decrease of its carrier density. In a ballistic system, these electrons are reflected back and do not contribute to the current, thereby generating LS resistance in the sample's bulk. In contrast, in the hydrodynamic regime electron-electron scattering transfers these electrons into transmitted channels, thus avoiding their reflection and the corresponding resistance.

Equipped with this analysis, we can raise the question of the minimal resistance of hydrodynamic electrons flowing through a constriction. In the ballistic case, for a sample of length L and a minimal cross section $2\pi r_{\min}$, the LS resistance is given by $(h/2e^2k_F r_{\min})$ (k_F is the Fermi momentum, and we consider a single spin species). In the hydrodynamic case, previous works [29,30,42] reported a reduction of the LS resistance by a factor of $\ell_{ee}/r_{\min}$ due to electron hydrodynamics. We find a further reduction of the resistance by an additional factor of $r_{\min}/L$ if the constriction's width varies over a scale $L \gg r_{\min}$. In contrast to the familiar ohmic regime, in which resistance increases with L, the resistance in the hydrodynamic regime decreases with L. This implies that a system with a given $r_{\min}$ and a large enough L may have an arbitrarily small total resistance.

Wormhole geometry.—In order to study the resistance of hydrodynamic electrons in a generic expanding geometry while avoiding boundary effects, we use a "wormhole"

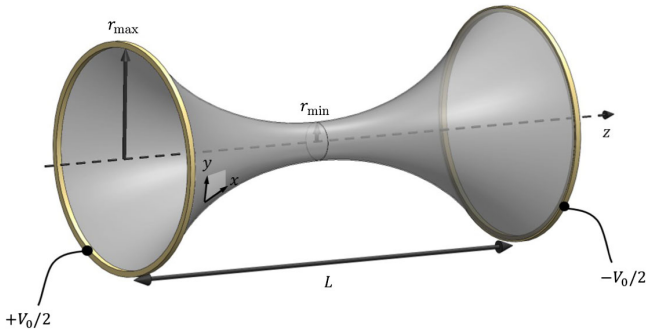

FIG. 1. The wormhole geometry is a two-dimensional azimuthally symmetric electronic system embedded in three-dimensional space, described by the equation $r = r(z)$, where the radius is maximal ($r_{\max}$) at the interface to the contacts and minimal ($r_{\min}$) at the center. A current I is driven from negative to positive z, and the potentials at the two contacts are $V(\mp L/2) = \pm(V_0/2)$.

geometry (Fig. 1). This geometry is a two-dimensional surface of revolution embedded in three dimensions, with azimuthal symmetry (toward the end of this Letter we consider also a Corbino disk and a bar with varying electronic density). In cylindrical coordinates the wormhole is defined by $r = r(z)$, with its minimum radius, $r_{\min}$, occurring at $z = 0$, and maximum radius, $r_{\max}$, occurring at the contacts positioned at $z = \pm L/2$. For simplicity we assume $r(z) = r(-z)$. A current I driven through the wormhole in the z direction leads to a potential $V(z = \mp L/2) = \pm(V_0/2)$ at its contacts. On the manifold, we define a local Cartesian system of coordinates tangent to the manifold, in which $\hat{y}$ is the unit vector in the azimuthal direction, and $\hat{x} = (1/\sqrt{1+r'2})(r', 0, 1)$ is the unit vector in the direction along the manifold. For brevity, we set $\hbar = e = 1$.

Boltzmann description.—Time-independent transport in a wormhole geometry may be described by a Boltzmann equation. In the absence of a driving force, the magnitude of the electron's momentum is constant, but its direction varies. Consequently, the equation reads as follows:

$$\cos\theta\partial_z f - \frac{r'}{r}\sin\theta\partial_\theta f = \sqrt{1+r'^2}I[f], \tag{1}$$

where $f(\boldsymbol{r},\boldsymbol{p})$ is the deviation of the number of electrons in a position $\boldsymbol{r}$ with momentum $\boldsymbol{p}$ from its equilibrium value, θ is the angle of the momentum with respect to the locally defined x direction, $r' \equiv dr/dz$, and $I[f]$ is the scattering integral, elaborated below. As explained in the Supplemental Material [54], this equation is derived in two steps. First, we solve for the trajectories of free particles constrained to the manifold. Second, we equate the variation of f along these trajectories with the scattering integral $I[f]$.

It is common to substitute the ansatz

$$f(\boldsymbol{p},\boldsymbol{r}) = \delta[\epsilon_F - \epsilon(\boldsymbol{p})]h(\boldsymbol{p},\boldsymbol{r}) \tag{2}$$

in Eq. (1), and integrate both sides over the magnitude of the momentum $\int(p\,dp/4\pi^2)$, with $p = |\boldsymbol{p}|$. This integration fixes $|\boldsymbol{p}| = p_F$ such that h becomes a function of $\boldsymbol{r}$ and θ, which describes the nonequilibrium angular shape of the Fermi surface. The integration replaces the δ function in Eq. (2) by a density of states at the Fermi energy and angle θ, $\nu(E_F,\theta) = \nu_F/2\pi$ (here, ν_F is the density of states at the Fermi energy). The Boltzmann equation becomes an equation for $\nu_F h(\theta,\boldsymbol{r})/2\pi$. The azimuthal symmetry reduces the dependence on $\boldsymbol{r}$ to a dependence on z only.

Landauer description.—In the Landauer picture, the system is composed of $2j_{\max}+1$ channels, enumerated by their angular momentum $j = -j_{\max}..0..j_{\max}$, with $j_{\max} = k_F r_{\max}$. The angular momentum $j = p_y(z)r(z)$, with p_y the momentum in the azimuthal direction. Each channel is characterized by transmission and reflection probabilities T_j, R_j satisfying $T_j + R_j = 1$. We assume $r(z)$ to vary slowly on the scale of the Fermi wavelength, such that in the absence of interactions, channels with $|j| < k_F r_{\min}$ are fully transmitted, and all other channels are fully reflected. The reflection takes place at the classical turning point $r(z) = |j|/k_F$. The current flowing through the wormhole is $I = (k_F r_{\min}/\pi)V_0$, leading to a dimensionless LS resistance $R_{\text{ballistic}} = \pi/k_F r_{\min}$.

"Landauerizing" Boltzmann.—We reformulate the Boltzmann equation to elucidate its relation to the Landauer picture. To that end, we express the shape of the Fermi surface in terms of different variables: the channel angular momentum j, the direction of motion, right (R) or left (L), and the position, z. Semiclassically, the angular momentum is a real number, which is quantized to an integer in Landauer's quantum mechanical analysis. Here, we think about it semiclassically.

Two steps are needed to transform the Boltzmann equation from an equation for $h(\theta,z)$ to an equation for the occupation in terms of j, z and direction of motion, which we denote by $h^j_{R,L}(z)$. First, we change the variables in Eq. (1). Second, the integral $\int(\text{pdp}/4\pi^2)$ should be replaced by an integral over the x component of the momentum, namely $p_F\int(dp_x/2\pi)$, where the limits are given by $p_x = 0$ and $p_x = \pm\infty$ for R and L, respectively. The δ function in Eq. (2) is then replaced by a density of states at the Fermi level at a fixed $j = p_y r(z)$:

$$\nu^j = \frac{\nu_F}{\sqrt{1-\left(\frac{j}{k_F r(z)}\right)^2}}\Theta(k_F r(z) - |j|). \tag{3}$$

This density of states is inversely proportional to the x component of the velocity, as familiar from Landauer's analysis. The details of the transformation are given in the Appendix, but the outcome is quite expected from the conservation of angular momentum:

$$\pm\nu_F \partial_z h^j_{R,L}(z) = \sqrt{1+r'^2}\,\tilde{I}[h^j_{R,L}(z)], \tag{4}$$

where the $\pm$ refers to right and left moving electrons, and $\tilde{I}$ is the scattering term expressed as a functional of $h^j_{R,L}(z)$, derived below.

The electronic density $\rho(z)$, current density $J_x(z)$, and potential $V(z)$ are

$$\begin{aligned}\rho(z) &= \int \frac{d\boldsymbol{p}}{4\pi^2} f(\boldsymbol{p},z) = \frac{1}{2\pi k_F r(z)} \int dj \nu^j(z)[h^j_R + h^j_L] \\ J_x(z) &= \int \frac{d\boldsymbol{p}}{4\pi^2}\frac{p_x}{m} f(\boldsymbol{p},z) = \frac{1}{4\pi^2 r(z)} \int dj [h^j_R - h^j_L] \\ V(z) &= \rho(z)/\nu_F,\end{aligned} \tag{5}$$

where the limits of integration are over all angular momenta for which $\nu^j \neq 0$, i.e., from $-j_{\max}$ to $j_{\max} = k_F r_{\max}$.

Ballistic regime.—In the absence of collisions ($\tilde{I} = 0$), Eq. (4) implies that $h^j_{R,L}$ is independent of z and is such that $h^j_R = h^j_L$ at the classical turning point, where $j = k_F r(z)$. The solution states that there is no interchannel scattering along the wormhole, which is a consequence of angular momentum conservation. As for intrachannel backscattering, two situations may exist. Fully transmitted channels are those with $j < k_F r_{\min}$. For these channels, each of the two nonequilibrium occupations $h^j_{R,L}(z)$ is determined by the contact from which it emanates, and is independent of z. In contrast, if there is a point z_0 for which $j = k_F r(z_0)$, at this point the momentum has no x component, $h_R = h_L$ and the channel is fully reflected. Then, on one side of z_0 where the channel exists we have $h_R = h_L$, with the value being determined by the contact from which the channel emanates and to which it is back-reflected. Both occupations vanish at the other side of z_0, in which the channel does not exist. Figures 2(a) and 2(b) present $h^j_R \mp h^j_L$ for a particular example of a ballistic wormhole, showing the nonequilibrium channel-dependent contributions to the local potential and current density.

Each contact feeds into the wormhole all channels below its potential, $\pm V_0/2$ for the left and right contacts, respectively, thus specifying the boundary conditions. By Landauer's formula, $V_0 = \pi I/k_F r_{\min}$. With these boundary conditions, we can solve for $h^j_{R,L}(z)$ and use the solution to calculate the potential as a function of z. We find the potential to be as follows:

$$\begin{aligned}V_{\text{ballistic}}(z) &= -\operatorname{sgn}(z)\frac{V_0}{\pi}\int_{k_F r_{\min}}^{k_F r(z)} \frac{dj}{\sqrt{[k_F r(z)]^2 - j^2}} \\ &= -\operatorname{sgn}(z)\frac{V_0}{2}\left[1 - \frac{2}{\pi}\arcsin\frac{r_{\min}}{r(z)}\right].\end{aligned} \tag{6}$$

Interestingly, although there are no collisions, we see that there is a potential drop, and thus resistance, in the bulk of the wormhole. Equation (6) shows that the potential close to the edges of the wormhole ($z = \pm L/2$) is smaller than that in the contacts by $(V_0/\pi)\arcsin(r_{\min}/r_{\max})$. This difference is the LS contact resistance. In the limit $r_{\max} \gg r_{\min}$ this contact resistance becomes negligible, and practically all the LS resistance drops in the bulk. From Eq. (6) we see that voltage drops in the bulk when the upper limit of the integral varies with z. Hence, the bulk LS resistance appears whenever the number of conduction channels varies in the bulk. As we show below, electron-electron scattering can dramatically suppress the bulk potential drop, allowing the system to conduct much better than the fundamental LS limit.

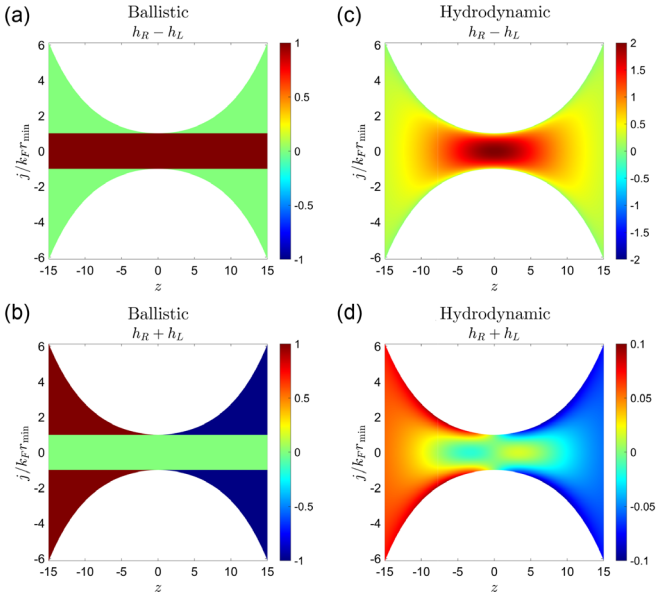

FIG. 2. Nonequilibrium distribution functions $h_R - h_L$ and $h_R + h_L$ for ballistic (a),(b) and hydrodynamic (c) and (d) cases. These distribution functions contribute to the current density and voltage, respectively [see Eq. (5)]. They are plotted for the wormhole defined in Eq. (11) with $a/r_0 = 6$, as a function of the spatial coordinate z, and the normalized channel index, $j/k_F r_{\min}$. In panels (c),(d) $\ell_{ee}/r_0 = 0.3$. Green color corresponds to zero population, while white reflects states above the Fermi energy.

Electron-electron scattering and the hydrodynamic regime.—We now turn to consider the effect of momentum conserving electron-electron interactions on the wormhole resistance. Within the relaxation time approximation, taking conservation laws into account [11,55], we have

$$I[f(\boldsymbol{p},\boldsymbol{r})] = -\frac{1}{\ell_{ee}}\left\{f - \frac{\delta[\epsilon_F - \epsilon(\boldsymbol{p})]}{\nu_F}\left[\rho(\boldsymbol{r}) + \frac{2J_x(\boldsymbol{r})\cos\theta}{v_F}\right]\right\}. \tag{7}$$

The second and third terms on the right-hand side guarantee charge and momentum conservation, respectively. We obtain $\tilde{I}[h^j]$ using the same ansatz we used before:

$$\tilde{I}[h^j_{R,L}(z)] = -\frac{\nu^j}{\ell_{ee}}\left[h^j_{R,L}(z) - \frac{\rho(z)}{\nu_F} \mp \frac{4\pi J_x(z)}{k_F}\sqrt{1-\left(\frac{j}{k_F r(z)}\right)^2}\right]. \tag{8}$$

The ν^j/ℓ_{ee} factor makes the mean free path j-dependent and shortens it from ℓ_{ee} to $\ell_{ee}\sqrt{1-[j/k_F r(z)]^2}$. This may be understood by noting that for $j/r(z)$ large, p_x is small and a shorter distance is traversed in the z direction between two scattering events. In particular, the scattering length vanishes when the channel is about to be terminated, opening a way for the electrons to avoid backscattering by being scattered to a transmitted channel. Furthermore, in contrast to the case of impurity scattering, in which in Eq. (8) ℓ_{ee} is replaced by a momentum-relaxing mean free path and the third term is absent, here the presence of the third term allows for a Galilean boost of the Fermi surface $h^j{}_{R,L}(z) = \pm[4\pi J_x(z)/k_F]\sqrt{1-[j/k_F r(z)]^2}$ to be carried out without developing a resistance.

We find the solution to a leading order in ℓ_{ee} (the calculation is given in the Appendix),

$$\begin{aligned} h^j_{R,L}(z) = {} & \pm\frac{2I}{k_F r(z)}\sqrt{1-\left[\frac{j}{k_F r(z)}\right]^2} \\ & + \frac{2I\ell_{ee}\sin\xi(z)}{k_F r^2(z)}\left\{1-2\left[\frac{j}{k_F r(z)}\right]^2\right\} \\ & - \int_0^z \frac{I\ell_{ee}}{k_F r^2(z')}\cos\xi(z')\frac{d\xi}{dz'}(z')dz', \end{aligned} \tag{9}$$

where $\xi(z)$ is the local angle between z axis and the manifold, i.e., $r(z)' = \tan\xi(z)$. This solution is valid in the bulk, away from the contacts. We comment on the role of the contacts below, with details in the Appendix.

The first term in Eq. (9) is a rigidly shifted Fermi surface. It is the solution expected for $r' = 0$ far away from the contacts, after all deformations of the Fermi surface are suppressed by the scattering term. The second and third terms are smaller than the first by a factor of $\ell_{ee}/r(z)$, and originate from the breaking of Galilean invariance. The second term makes the shifted Fermi surface acquire an elongated shape, with more electrons in the head-on direction (small j), and less in the $j \approx k_F r(z)$ channels. The third term is independent of j. It carries an electronic density, and leads to a potential drop and resistivity. Note that while the second term exists when $\sin\xi \neq 0$, the third term requires $(d\sin\xi/dz) \neq 0$. Stated differently, in contrast to ballistic electrons for which local resistance appears when the number of conduction channels varies with z, i.e., when $r' \neq 0$, for hydrodynamic electrons resistance is generated only when this function has a nonzero curvature, $r'' \neq 0$.

The potential originating from the third term of Eq. (9) may be written also as follows:

$$V_{\text{hydro}}(z) = I\int_0^{\xi(z)} \frac{\ell_{ee}}{4\pi k_F r^2(\xi)}\cos\xi d\xi. \tag{10}$$

The resistance scale may be estimated from Eq. (10). The r^2 in the denominator suggests that the wormhole resistance is characterized by a "superballistic" scale [29,30,42,50], $(2\pi\ell_{ee}/k_F r^2_{\min})$, smaller by $2\ell_{ee}/r_{\min}$ than the ballistic LS resistance. However, Eq. (10) opens the way for a much smaller scale, $(\ell_{ee}/4\pi k_F r^2_{\min})\sin\xi_0$, where ξ_0 is the angle at which r becomes much larger than $r_{\min}$. If r grows slowly, $\sin\xi_0$ may be much smaller than 1, with the resistance becoming much smaller than the superballistic scale. Consequently, for a fixed $r_{\max} \gg r_{\min}$ the resistance generally decreases with increasing L, opposite to the familiar Ohmic dependence.

To illustrate the two hydrodynamic scales, consider an example where

$$r(z) = r_0\cosh z/a. \tag{11}$$

In this wormhole, $r_{\min} = r_0$ and $r_{\max} \gg r_{\min}$ for $L \gg a$. Under the latter condition, the contribution to the resistance decays fast with $|z| \gg a$, and we can take $L \to \infty$. Then, using Eq. (10),

$$R_{\cosh} = \frac{\ell_{ee}}{2\pi k_F}\left[\frac{1}{r_0^2-a^2} - \frac{a^2 \operatorname{arctanh}\frac{\sqrt{r_0^2-a^2}}{r_0}}{r_0(r_0^2-a^2)^{3/2}}\right]. \tag{12}$$

In the limit $a \to 0$ the resistance tends to $(\ell_{ee}/2\pi k_F r_0^2)$, but when $a \gg r_0$ it decreases to become of order $(\ell_{ee}/4k_F r_0 a)$. As can be seen in Eq. (10), most of the resistance originates from the product of the minimum radius $r_{\min}$ and the change in angle $\Delta\xi$ over which the radius becomes significantly larger than r_0. When $a \gg r_0$ the change in angle is $\Delta\xi \sim r_0/a$ and hence the decrease in resistance. Figures 2(c) and 2(d) show the calculated $h_L - h_R$ and $h_L + h_R$ for hydrodynamic flow in the wormhole in Eq. (11). These quantities contribute to the current density and potential, respectively [Eq. (5)]. Figure 3 shows potential drop in this wormhole as a function of z, in the ballistic case and in the hydrodynamic cases for two values of a/r_0. The hydrodynamic suppression of the resistance with increasing a is evident. Note that when $r(z)$ is constant the resistance in the bulk vanishes, since the bulk is Galilean invariant. However, the LS voltage drop occurs then sharply at the contacts, and is not suppressed by electron-electron scattering. To suppress the resistance by electron-electron scattering $r(z)$ should vary slowly from $r_{\min}$ to $r_{\max} \gg r_{\min}$.

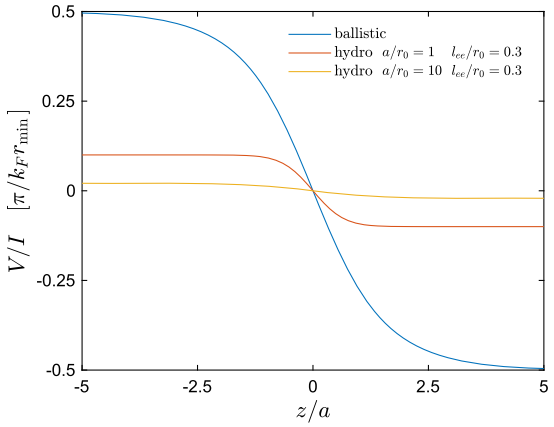

FIG. 3. The potential along the wormhole defined in Eq. (11), divided by the current, V/I, in units of the LS resistance, plotted for a ballistic flow ($\ell_{ee} = \infty$) and hydrodynamic flows ($\ell_{ee}/r_{\min} = 0.3$) with varying values of a/r_0 (see legend).

Our analysis elucidates this suppression of the resistance: a potential drop results from reflection of electrons. In the ballistic regime the contact sends into the sample electrons for which j is too large to be transmitted. Those electrons are reflected, leading to a voltage drop [Eq. (6)]. In contrast, in the hydrodynamic regime electrons of high j are scattered to channels of smaller j, and largely end up being transmitted, without generating a potential drop. Note that our entire analysis assumes $\ell_{ee} \ll a$ and $\ell_{ee} \ll r_0$, in contrast to the sharp constriction case, studied, e.g., in [29], leading to a rather different evolution of R with ℓ_{ee}.

Equations (10) and (11) show that the bulk resistance of a Corbino disk vanishes, as a consequence of the lack of variation of ξ. With the limitation of z to a proper range, and with the limit $a \to 0$, Eq. (11) may be used to describe a Corbino disk. The resulting bulk resistance vanishes in that limit. Indeed, in a Corbino disk the number of channels grows linearly with the radial coordinate, its second derivative vanishes, and so does the hydrodynamic resistance. Importantly, this vanishing bulk resistance is in series with a contact resistance which in this case is $\pi/(2k_F r_{\min})$, where $r_{\min}$ is the inner radius of the disk.

The elimination of the LS resistance in a Corbino disk was experimentally confirmed, as reported in a companion article [56]. In that article, we generalized the present calculations to include momentum relaxation due to phonon and impurity scattering, and showed that it leads to a simple additive contribution to the resistance.

Finally, although the wormhole is illuminating theoretically, it is a rather exotic geometry for real-life transistor devices. Those typically have a long rectangular bar geometry, in which the density varies along the x axis and is maximal near the contacts. In a bar geometry, previous work (e.g., [27]) has focused on a viscous contribution arising from the no-slip boundary condition. Here, we neglect this contribution by assuming specular boundary scattering, or a wide bar. By carrying out an analysis similar to that of the wormhole (see the Supplemental Material [54]**), we find the resistance

$$R_{\text{bar}} = \int_{-\infty}^{\infty} dx \frac{(k_F' \ell_{ee})'}{2k_F^2 r}. \tag{13}$$

Here, we account also for the possibility that ℓ_{ee} varies with the variation of k_F. Assuming that the change in k_F is much larger than its minimal value, we can estimate $R \sim \ell_{ee}/k_F r a$, where a is the scale over which k_F and ℓ_{ee} become much larger than their minimal value.

In summary, we showed here that when the LS resistance of an electronic system is spread into its bulk, rather than being localized at the interface with the contacts, it may be significantly reduced by electron-electron scattering, in principle all the way down to zero.

We thank L. Ella, G. Falkovich, L. Levitov, M. Polini, M. Shavit, A. Rozen, A. V. Shytov and U. Zondiner for useful discussions. Work was supported by the Leona M. and Harry B. Helmsley Charitable Trust grant, ISF grant (No. 1182/21), Minerva grant (No. 713237), Hydrotronics (No. 873028) and the ERC-Cog (See-1D-Qmatter, No. 647413). T. S. acknowledges the support of the Natural Sciences and Engineering Research Council of Canada (NSERC), in particular the Discovery Grant (No. RGPIN-2020-05842), the Accelerator Supplement (No. RGPAS-2020-00060) and the Discovery Launch Supplement (No. DGECR-2020-00222). This research was enabled in part by support provided by Compute Canada. A. S. was supported by the ERC under the Horizon 2020 Research and Innovation programme (LEGOTOP No. 788715), the DFG (CRC/Transregio 183, EI 519/7-1), and the ISF Quantum Science and Technology (2074/19).

[1] R. Landauer, IBM J. Res. Dev. **1**, 223 (1957).
[2] Y. V. Sharvin, Sov. J. Exp. Theor. Phys. **21**, 655 (1965).
[3] S. Datta, *Electronic Transport in Mesoscopic Systems*, Cambridge Studies in Semiconductor Physics and Microelectronic Engineering (Cambridge University Press, Cambridge, England, 1995).
[4] Y. Imry, *Introduction to Mesoscopic Physics* (Oxford University Press on Demand, New York, 2002).
[5] R. Gurzhi, Sov. Phys. JETP **44**, 771 (1963).
[6] R. Gurzhi, Phys.-Usp. **11**, 255 (1968).
[7] J. E. Black, Phys. Rev. B **21**, 3279 (1980).
[8] Z. Z. Yu, M. Haerle, J. W. Zwart, J. Bass, W. P. Pratt, and P. A. Schroeder, Phys. Rev. Lett. **52**, 368 (1984).
[9] R. N. Gurzhi, A. N. Kalinenko, and A. I. Kopeliovich, Phys. Rev. Lett. **74**, 3872 (1995).
[10] L. W. Molenkamp and M. J. M. de Jong, Phys. Rev. B **49**, 5038 (1994).
[11] M. J. M. de Jong and L. W. Molenkamp, Phys. Rev. B **51**, 13389 (1995).

[12] M. Dyakonov and M. Shur, Phys. Rev. Lett. **71**, 2465 (1993).
[13] E. Chow, H. P. Wei, S. M. Girvin, and M. Shayegan, Phys. Rev. Lett. **77**, 1143 (1996).
[14] B. Spivak and S. A. Kivelson, Ann. Phys. (Amsterdam) **321**, 2071 (2006).
[15] A. V. Andreev, S. A. Kivelson, and B. Spivak, Phys. Rev. Lett. **106**, 256804 (2011).
[16] I. Torre, A. Tomadin, A. K. Geim, and M. Polini, Phys. Rev. B **92**, 165433 (2015).
[17] P. S. Alekseev, Phys. Rev. Lett. **117**, 166601 (2016).
[18] A. Tomadin, G. Vignale, and M. Polini, Phys. Rev. Lett. **113**, 235901 (2014).
[19] L. Levitov and G. Falkovich, Nat. Phys. **12**, 672 (2016).
[20] A. Principi, G. Vignale, M. Carrega, and M. Polini, Phys. Rev. B **93**, 125410 (2016).
[21] M. Sherafati, A. Principi, and G. Vignale, Phys. Rev. B **94**, 125427 (2016).
[22] H. Guo, E. Ilseven, G. Falkovich, and L. Levitov, arXiv:1612.09239.
[23] A. Lucas, Phys. Rev. B **95**, 115425 (2017).
[24] A. Levchenko, H.-Y. Xie, and A. V. Andreev, Phys. Rev. B **95**, 121301(R) (2017).
[25] D. A. Bandurin, I. Torre, R. K. Kumar, M. Ben Shalom, A. Tomadin, A. Principi, G. H. Auton, E. Khestanova, K. S. Novoselov, I. V. Grigorieva, L. A. Ponomarenko, A. K. Geim, and M. Polini, Science **351**, 1055 (2016).
[26] J. Crossno, J. K. Shi, K. Wang, X. Liu, A. Harzheim, A. Lucas, S. Sachdev, P. Kim, T. Taniguchi, K. Watanabe, T. A. Ohki, and K. C. Fong, Science **351**, 1058 (2016).
[27] P. J. W. Moll, P. Kushwaha, N. Nandi, B. Schmidt, and A. P. Mackenzie, Science **351**, 1061 (2016).
[28] B. N. Narozhny, I. V. Gornyi, A. D. Mirlin, and J. Schmalian, Ann. Phys. (Berlin) **529**, 1700043 (2017).
[29] H. Guo, E. Ilseven, G. Falkovich, and L. S. Levitov, Proc. Natl. Acad. Sci. U.S.A. **114**, 3068 (2017).
[30] R. Krishna Kumar, D. A. Bandurin, F. M. D. Pellegrino, Y. Cao, A. Principi, H. Guo, G. H. Auton, M. Ben Shalom, L. A. Ponomarenko, G. Falkovich, K. Watanabe, T. Taniguchi, I. V. Grigorieva, L. S. Levitov, M. Polini, and A. K. Geim, Nat. Phys. **13**, 1182 (2017).
[31] T. Scaffidi, N. Nandi, B. Schmidt, A. P. Mackenzie, and J. E. Moore, Phys. Rev. Lett. **118**, 226601 (2017).
[32] A. Lucas and S. A. Hartnoll, Phys. Rev. B **97**, 045105 (2018).
[33] D. Y. H. Ho, I. Yudhistira, N. Chakraborty, and S. Adam, Phys. Rev. B **97**, 121404(R) (2018).
[34] A. Shytov, J. F. Kong, G. Falkovich, and L. Levitov, Phys. Rev. Lett. **121**, 176805 (2018).
[35] P. S. Alekseev and M. A. Semina, Phys. Rev. B **98**, 165412 (2018).
[36] D. Svintsov, Phys. Rev. B **97**, 121405(R) (2018).
[37] J. Gooth, F. Menges, N. Kumar, V. Süss, C. Shekhar, Y. Sun, U. Drechsler, R. Zierold, C. Felser, and B. Gotsmann, Nat. Commun. **9**, 4093 (2018).
[38] B. A. Braem, F. M. D. Pellegrino, A. Principi, M. Röösli, C. Gold, S. Hennel, J. V. Koski, M. Berl, W. Dietsche, W. Wegscheider, M. Polini, T. Ihn, and K. Ensslin, Phys. Rev. B **98**, 241304(R) (2018).
[39] A. I. Berdyugin, S. G. Xu, F. M. D. Pellegrino, R. Krishna Kumar, A. Principi, I. Torre, M. Ben Shalom, T. Taniguchi, K. Watanabe, I. V. Grigorieva, M. Polini, A. K. Geim, and D. A. Bandurin, Science **364**, 162 (2019).
[40] J. A. Sulpizio, L. Ella, A. Rozen, J. Birkbeck, D. J. Perello, D. Dutta, M. Ben-Shalom, T. Taniguchi, K. Watanabe, T. Holder, R. Queiroz, A. Principi, A. Stern, T. Scaffidi, A. K. Geim, and S. Ilani, Nature (London) **576**, 75 (2019).
[41] B. N. Narozhny, Ann. Phys. (Amsterdam) **411**, 167979 (2019).
[42] M. Shavit, A. Shytov, and G. Falkovich, Phys. Rev. Lett. **123**, 026801 (2019).
[43] M. J. H. Ku, T. X. Zhou, Q. Li, Y. J. Shin, J. K. Shi, C. Burch, L. E. Anderson, A. T. Pierce, Y. Xie, A. Hamo, U. Vool, H. Zhang, F. Casola, T. Taniguchi, K. Watanabe, M. M. Fogler, P. Kim, A. Yacoby, and R. L. Walsworth, Nature (London) **583**, 537 (2020).
[44] A. Levchenko and J. Schmalian, Ann. Phys. (Amsterdam) **419**, 168218 (2020).
[45] T. Holder, R. Queiroz, T. Scaffidi, N. Silberstein, A. Rozen, J. A. Sulpizio, L. Ella, S. Ilani, and A. Stern, Phys. Rev. B **100**, 245305 (2019).
[46] A. Jenkins, S. Baumann, H. Zhou, S. A. Meynell, D. Yang, K. Watanabe, T. Taniguchi, A. Lucas, A. F. Young, and A. C. Bleszynski Jayich, arXiv:2002.05065.
[47] A. C. Keser, D. Q. Wang, O. Klochan, D. Y. H. Ho, O. A. Tkachenko, V. A. Tkachenko, D. Culcer, S. Adam, I. Farrer, D. A. Ritchie, O. P. Sushkov, and A. R. Hamilton, Phys. Rev. X **11**, 031030 (2021).
[48] A. Gupta, J. J. Heremans, G. Kataria, M. Chandra, S. Fallahi, G. C. Gardner, and M. J. Manfra, Phys. Rev. Lett. **126**, 076803 (2021).
[49] Z. J. Krebs, W. A. Behn, S. Li, K. J. Smith, K. Watanabe, T. Taniguchi, A. Levchenko, and V. W. Brar, arXiv:2106.07212.
[50] Q. Hong, M. Davydova, P. J. Ledwith, and L. Levitov, arXiv:2012.03840.
[51] K. E. Nagaev and O. S. Ayvazyan, Phys. Rev. Lett. **101**, 216807 (2008).
[52] K. E. Nagaev and T. V. Kostyuchenko, Phys. Rev. B **81**, 125316 (2010).
[53] M. Y. Melnikov, J. P. Kotthaus, V. Pellegrini, L. Sorba, G. Biasiol, and V. S. Khrapai, Phys. Rev. B **86**, 075425 (2012).
[54] See Supplemental Material at http://link.aps.org/supplemental/10.1103/PhysRevLett.129.157701 for (A) a derivation of the Bolzmann equation in a wormhole geometry, (B) a solution of the Boltzmann equation in the hydrodynamic regime for a wormhole and Corbino geometry, (C) a solution of the Boltzmann equation in the hydrodynamic regime for a bar geometry with a density variation, (D) a calculation of the contact resistance.
[55] J. Callaway, Phys. Rev. **113**, 1046 (1959).
[56] C. Kumar, J. Birkbeck, J. A. Sulpizio, D. J. Perello, T. Taniguchi, K. Watanabe, O. Reuven, T. Scaffidi, A. Stern, A. K. Geim, and S. Ilani, Nature **609**, 276 (2022).